# Pair production of neutralinos and charginos at the LHC: The role of Higgs bosons exchange

Abdesslam Arhrib,[1,2,3] Rachid Benbrik,[3,4,5] Mohamed Chabab,[3] and Chuan-Hung Chen[6,1]

[1]*Department of Physics, National Cheng-Kung University, Tainan 701, Taiwan*
[2]*Faculté des Sciences et Techniques, B. P 416 Tangier, Morocco*
[3]*LPHEA, FSSM, Cadi Ayyad University, B. P. 2390, Marrakesh, Morocco*
[4]*Instituto de Física de Cantabria (CSIC-UC), Santander, Spain*
[5]*Faculté Polydisciplinaire de Safi, Sidi Bouzid B. P 4162, 46000 Safi, Morocco*
[6]*National Center for Theoretical Sciences, Hsinchu 300, Taiwan*

(Received 8 September 2011; published 14 December 2011)

We analyze the effects of the $s$-channel Higgs bosons exchange on the charginos-pair and neutralinos-pair production in proton-proton collision at the CERN Large Hadron Collider (LHC) in the following channels: $pp \to \tilde{\chi}^+\tilde{\chi}^-/\tilde{\chi}^0\tilde{\chi}^0 + X$, within the minimal supersymmetric standard model (MSSM). Assuming the usual GUT relation between $M_1$ and $M_2$ at the weak scale, we found that substantial enhancement can be obtained through $s$-channel Higgs bosons exchange in the mixed regime where $M_2 \sim |\mu|$ with moderate to large $\tan\beta$ at the resonance of the heavy Higgs bosons. By combining the phenomenological constraints on neutralinos and charginos, we may still find regions of parameter space where charginos-pair and neutralinos-pair production at the LHC from $b\bar{b}$ initial state can be large and observable at LHC. We also compute the full complete set of electroweak (EW) contributions to $pp \to gg \to \tilde{\chi}^+\tilde{\chi}^-/\tilde{\chi}^0\tilde{\chi}^0 + X$ at the one-loop level in the general MSSM. The analytical computation of the complete tree-level amplitude for $b\bar{b} \to \tilde{\chi}^+\tilde{\chi}^-/\tilde{\chi}^0\tilde{\chi}^0 + X$, including $s$-channel Higgs exchange, is given.

DOI: 10.1103/PhysRevD.84.115012 PACS numbers: 12.60.Jv, 14.80.Nb

## I. INTRODUCTION

The standard model (SM) [1,2,5], a theory of strong and electroweak interactions, is amazingly consistent with most precision measurements up to the present accessible energies. Nevertheless, the notorious hierarchy problem indicates that the SM should be an effective theory at electroweak scale. One of the solutions to the hierarchy problem is to introduce supersymmetry (SUSY), where the quadratic divergences induced by one-loop corrections to Higgs mass are smeared. Therefore, the important extension of the SM in the framework of SUSY is the minimal supersymmetric standard model (MSSM). If we further impose a discrete $R$-parity $R_p = (-1)^{2S+3(B+L)}$ [6–10] to the system, where the super particles carry odd $R$-parity and $S$, $B$, and $L$ denotes the spin, baryon, and lepton number of a particle, respectively, a stable lightest supersymmetric particle (LSP) exists and the superpartners of the SM particles are always produced in pairs.

Motivated by the existence of dark matter (DM) that has the abundance of 24% in the universe, the neutral stable LSP might be considered as a DM candidate [11]. Although sneutrino, the superpartner of neutrino, could be a viable candidate of DM, enormous studies are concentrated on the neutralino, where the state consists of neutral gauginos and higgsinos [12]. The interest to adopt neutralino as LSP in the MSSM is that the corresponding mass matrix in interaction eigenstates only depends on four unknown parameters: $M_{1,2}$, $\mu$, and $\tan\beta = v_2/v_1$, where $M_{1[2]}$ is soft SUSY-breaking gaugino mass of $SU(1)[(2)]$ gauge symmetry, $\mu$ is the mixing coefficient of doublets $\phi_u$ and $\phi_d$ in Higgs potential, and $v_{1(2)}$ is the vacuum expectation value (VEV) of $\phi_{d(u)}$. Hence, if the neutralino is observed, it not only confirms SUSY, but also provides the clue of DM. Additionally, due to the similarity in involved parameters, the possible next LSP could be the chargino, which consists of charged gauginos and higgsinos. For completeness, in this paper we study various mechanisms for the production of charginos and neutralinos at the Large Hadron Collider (LHC) in detail.

In the literature, the studies of chargino/neutralino pair production in the MSSM are concentrated on the Drell-Yan process of quark-antiquark annihilation and gluon-gluon fusion. For instance, the direct production of charginos and neutralinos at Tevatron/LHC by $p\bar{p}/pp \to \tilde{\chi}_i\tilde{\chi}_j + X$ through quark-antiquark annihilation at the next-to-leading order (NLO) was investigated by Beenakker *et al.* [13]. The charginos and neutralinos pair production by gluon-gluon fusion were analyzed in Ref. [14,15] in the framework of mSUGRA model. The neutralino pair production via quark-antiquark annihilation at LHC was considered by Han *et al.* [16]. Moreover, the correlation of beam polarization and gaugino/higgsino mixing was studied in Ref. [17]. It is worth mentioning that although chargino/neutralino pair production by gluon fusion is loop effects, due to the high luminosity of LHC, the production rate can still be significant. One can also access chargino and neutralino pairs from Heavy Higgs bosons which could be copiously produced at LHC and followed by their subsequent decays into chargino and neutralino pairs. Detail studies of such scenario have been addressed in [18–20].

 

Beside the channels mentioned earlier, in this paper we are going to explore the case when the value of $\tan\beta$ is as large as that of $m_t/m_b$ and the production mechanism is through the annihilation of bottom-antibottom pair with scalar Higgs ($H^0, A^0$) as the mediator.[1] The reason to study such effect is because the involved coupling is associated with $m_b \tan\beta/v$ and $v = \sqrt{v_1^2 + v_2^2}$. Although the parton distribution function (PDF) of the bottom quark inside a proton is smaller than that of the light quark, interestingly, the chargino/neutralino production rate will be enhanced naturally in the scenario of large $\tan\beta$. Furthermore, we also find that another enhanced effect will be created when the mediated Higgs is tuned to be a resonant Higgs, i.e., the condition $\sqrt{p_b^2 + p_{\tilde{b}}^2} = \sqrt{\hat{s}} \approx m_{H^0,A^0} \approx 2m_{\tilde{\chi}}$ is satisfied. Intriguingly, the same resonant effect plays a prominent role in the neutralino DM, where the LSP neutralino yields the desired amount of relic density in some region of the SUSY parameter space [23].

The paper is organized as follows. In Sec. II, we introduce the basic properties of charginos and neutralinos and the radiative corrections to the bottom Yukawa coupling in the MSSM. In Sec. III, we present the production mechanisms for chargino/neutralino pair production via quark annihilation and gluon fusion and discuss the constraints on the SUSY parameters. We do the detailed numerical analysis on the production cross sections in Sec. IV. We give conclusions in Sec. V. Additionally, the relevant couplings of the chargino/neutralino to gauge bosons and Higgs bosons are given in Appendix A. The analytic expressions for chargino/neutralino pair production in the exchange of Higgs boson are summarized in Appendix B.

## II. MASSES AND YUKAWA COUPLINGS OF CHARGINOS AND NEUTRALINOS

For studying the production of charginos and neutralinos, we introduce the relevant properties of charginos and neutralinos in this section, whereas the details of the couplings of charginos/neutralinos to gauge bosons, Higgs bosons, fermions and sfermions are given in Appendix A. For comparing with the results in the literature, hereafter, we adopt the notation that was used in Refs. [12,24].

### A. Masses of charginos and neutralinos

In terms of two-component Weyl spinors, the chargino mass term in the Lagrangian could be described by

$$\mathcal{L}^{m}_{\tilde{\chi}^{\pm}} = -\frac{1}{2}(\psi^+ \psi^-)\begin{pmatrix} 0 & \mathcal{M}_C^T \\ \mathcal{M}_C & 0 \end{pmatrix}\begin{pmatrix} \psi^+ \\ \psi^- \end{pmatrix} + \text{H.c}, \quad (1)$$

where $\mathcal{M}_C$ is given by [24]

$$\mathcal{M}_C = \begin{pmatrix} M_2 & \sqrt{2}M_W s_\beta \\ \sqrt{2}M_W c_\beta & \mu \end{pmatrix} \quad (2)$$

with $s_\beta(c_\beta) \equiv \sin\beta(\cos\beta)$ and the representations of $\psi_j^{\pm}$ for winos and charged higgsinos are

$$\psi_j^+ = (-i\lambda^+, \psi^1_{H_2}), \quad \psi_j^- = (-i\lambda^-, \psi^2_{H_1}), \quad j = 1, 2. \quad (3)$$

Since the matrix $\mathcal{M}_C$ is not symmetric, for diagonalizing it, we need to introduce two $2 \times 2$ unitary matrices $U$ and $V$, i.e.

$$U^* \mathcal{M}_C V^{-1} = \text{diag}(m_{\tilde{\chi}_1^{\pm}}, m_{\tilde{\chi}_2^{\pm}}) \to U = \mathcal{O}_- \quad \text{and}$$
$$V = \begin{cases} \mathcal{O}_+ & \text{if } \det\mathcal{M}_C > 0, \\ \sigma_3 \mathcal{O}_+ & \text{if } \det\mathcal{M}_C < 0. \end{cases} \quad (4)$$

Here, the third Pauli matrix $\sigma_3$ is used to make the eigenvalues of $\mathcal{M}_C$ to be positive and $\mathcal{O}_\pm$ are the $2 \times 2$ rotational matrices in which the mixing angles are

$$\tan 2\theta_- = \frac{2\sqrt{2}M_W(M_2 c_\beta + \mu s_\beta)}{M_2^2 - \mu^2 - 2M_W^2 c_{2\beta}},$$
$$\tan 2\theta_+ = \frac{2\sqrt{2}M_W(M_2 s_\beta + \mu c_\beta)}{M_2^2 - \mu^2 + 2M_W^2 c_{2\beta}}. \quad (5)$$

Accordingly, the mass eigenstates of charginos could be expressed by

$$\tilde{\chi}_i^+ = V_{ij}\psi_j^+, \qquad \tilde{\chi}_i^- = U_{ij}\psi_j^- \quad (6)$$

and the corresponding mass eigenvalues are given by

$$m^2_{\tilde{\chi}^{\pm}_{1,2}} = \tfrac{1}{2}\Big[M_2^2 + \mu^2 + 2M_W^2 \mp \sqrt{(M_2^2 - \mu^2)^2 + 4M_W^2(M_W^2 c_{2\beta}^2 + M_2^2 + \mu^2 + 2M_2\mu s_{2\beta})}\Big].$$

If the lightest chargino mass $m_{\tilde{\chi}_1^{\pm}}$ is known, $|\mu|$ can be regarded as a function of $M_2$ and the angle $\beta$. In the limit $|\mu| \gg M_2, M_W$, the masses of charginos could be simplified as

$$m_{\tilde{\chi}_1^{\pm}} \simeq M_2 - \frac{M_W^2}{\mu^2}(M_2 + \mu s_{2\beta}),$$
$$m_{\tilde{\chi}_2^{\pm}} \simeq |\mu| + \frac{M_W^2}{\mu^2}\,\text{sign}(\mu)(M_2 s_{2\beta} + \mu). \quad (7)$$

Clearly, if $|\mu| \to \infty$, the light chargino corresponds to a pure wino state with $m_{\tilde{\chi}_1^{\pm}} \simeq M_2$, while the heavy

[1] Similar analysis has been done for squark pair production at LHC [21] and stau production at hadron colliders [22].

chargino corresponds to a pure higgsino state with $m_{\tilde{\chi}_2^+} = |\mu|$.

Next, we turn to discuss the case of the neutralinos. Since there are four neutral Weyl spinors, the mass term of neutralinos in the Lagrangian is written as

$$\mathcal{L}^{m}_{\tilde{\chi}^0} = -\frac{1}{2}(\psi_i^0)^T[\mathcal{M}_N]_{ij}\psi_j^0 + \text{H.c.}, \tag{8}$$

with

$$\begin{aligned}\psi_i^0 = (&-i\lambda_\gamma, -i\lambda_Z, \psi^1_{H_1}\cos\beta - \psi^2_{H_2}\sin\beta, \psi^1_{H_1}\sin\beta \\ &+ \psi^2_{H_2}\cos\beta), \\ i &= 1, \ldots, 4,\end{aligned} \tag{9}$$

where the Weyl spinor in above equation in turn is the photino, the zino and the neutral higgsinos. The matrix form of $\mathcal{M}_N$ is explicitly given by

$$\mathcal{M}_N = \begin{pmatrix} M_1 & 0 & -M_Z s_W c_\beta & M_Z s_W s_\beta \\ 0 & M_2 & M_Z c_W c_\beta & -M_Z c_W s_\beta \\ -M_Z s_W c_\beta & M_Z c_W c_\beta & 0 & -\mu \\ M_Z s_W s_\beta & -M_Z c_W s_\beta & -\mu & 0 \end{pmatrix}, \tag{10}$$

with $s_W(c_W) \equiv \sin\theta_W(\cos\theta_W)$ and $\theta_W$ being Weinberg angle. Since neutralinos are Majorana type fermions, the mass matrix $\mathcal{M}_N$ can be diagonalized by using only one unitary matrix $Z$. If we set the physical mass of neutralino $m_{\tilde{\chi}_i^0}$, then the $4 \times 4$ unitary matrix Z should satisfy [24]

$$Z^* \mathcal{M}_N Z^{-1} = \text{diag}(m_{\tilde{\chi}_1^0}, m_{\tilde{\chi}_2^0}, m_{\tilde{\chi}_3^0}, m_{\tilde{\chi}_4^0}). \tag{11}$$

Consequently, the relation between weak and physical eigenstates can be expressed as

$$\tilde{\chi}^0_n = Z_{ni}\psi^0_i. \tag{12}$$

Because the complete relation between $m_{\tilde{\chi}_i^0}$ and the parameters $M_{1,2}$, $\mu$ and $s_W(c_W)$ is complicated, the detailed expressions can be found in Ref. [25]. Nevertheless, if we take $|\mu| \gg M_{1,2}, M_Z$, the relations can be simplified as [26]

$$\begin{aligned} m_{\tilde{\chi}_1^0} &\simeq M_1 - \frac{M_Z^2}{\mu^2}(M_1 + \mu s_{2\beta})s_W^2, \\ m_{\tilde{\chi}_2^0} &\simeq M_2 - \frac{M_Z^2}{\mu^2}(M_2 + \mu s_{2\beta})c_W^2, \\ m_{\tilde{\chi}_3^0} &\simeq |\mu| + \frac{1}{2}\frac{M_Z^2}{\mu^2}\epsilon_\mu(1 - s_{2\beta})(\mu + M_2 s_W^2 + M_1 c_W^2), \\ m_{\tilde{\chi}_4^0} &\simeq |\mu| + \frac{1}{2}\frac{M_Z^2}{\mu^2}\epsilon_\mu(1 + s_{2\beta})(\mu - M_2 s_W^2 - M_1 c_W^2). \end{aligned} \tag{13}$$

We see clearly that the first two light neutralinos $\tilde{\chi}_1^0$ and $\tilde{\chi}_2^0$ are dominated by gauginos of $SU(1)$ and $SU(2)$, respectively, while the last two heavy neutralinos $\tilde{\chi}_{3,4}^0$ are aligned to the states of higgsinos.

### B. Yukawa couplings

It is now well established that the coupling of the $b - \bar{b} - H_k^0$ induces a modification of the tree-level relation between the bottom quark mass and its Yukawa coupling [27–30]. Those corrections are amplified at large $\tan\beta$. The modifications can be absorbed by redefining the bottom Yukawa coupling as

$$Y^b = \frac{\sqrt{2}m_b}{v\cos\beta} \to \frac{\sqrt{2}}{v\cos\beta}\frac{m_b}{1+\Delta_b} \approx \frac{\sqrt{2}}{v}\frac{m_b}{1+\Delta_b}\tan\beta, \tag{14}$$

where the second expression is valid for large $\tan\beta$ and the SUSY-QCD corrections lead to

$$\begin{aligned}\Delta_b = &\frac{2\alpha_s}{3\pi}\mu m_{\tilde{g}}\tan\beta I(m_{\tilde{b}_1}, m_{\tilde{b}_2}, m_{\tilde{g}}) \\ &+ \frac{(Y^t)^2}{16\pi^2}\mu A_t \tan\beta I(m_{\tilde{t}_1}, m_{\tilde{t}_2}, \mu),\end{aligned} \tag{15}$$

where $m_{\tilde{g}}$ denotes the gluino mass, and the function $I$ is given by

$$\begin{aligned} I(a,b,c) = &\frac{-1}{(a^2-b^2)(b^2-c^2)(c^2-a^2)} \\ &\times \left(a^2b^2\ln\frac{a^2}{b^2} + b^2c^2\ln\frac{b^2}{c^2} + c^2a^2\ln\frac{c^2}{a^2}\right). \end{aligned} \tag{16}$$

In $\Delta_b$ we only keep the dominant contributions from the gluino-sbottom and charged-higgsino-stop loops because they are proportional to the strong coupling and to the top Yukawa coupling, respectively, while neglecting those that are proportional to the weak gauge coupling. Note that $\Delta_b$ is evaluated at the scale of SUSY particles $M_{\text{SUSY}}$ where the heavy particles in the loop decouple, whereas the bottom Yukawa coupling $Y^b(Q)$ is determined by the running $b$-quark mass $m_b(Q)$ at the scale $Q$:

$$Y^b(Q) = \frac{\sqrt{2}m_b(Q)}{v\cos\beta}\frac{1}{1+\Delta_b(M_{\text{SUSY}})}. \tag{17}$$

The contributions to the bottom Yukawa couplings which are enhanced at large $\tan\beta$ can be included to all orders by making the following replacements [31,32]

$$g_{hbb} \to g_{hbb}\frac{1 - \Delta_b(M_{\text{SUSY}})/(\tan\beta\tan\alpha)}{1+\Delta_b(M_{\text{SUSY}})} \tag{18}$$

$$g_{Hbb} \to g_{Hbb}\frac{1 + \Delta_b(M_{\text{SUSY}})\tan\alpha/\tan\beta}{1+\Delta_b(M_{\text{SUSY}})} \tag{19}$$

$$g_{Abb} \to g_{Abb}\frac{1 - \Delta_b(M_{\text{SUSY}})/\tan^2\beta}{1+\Delta_b(M_{\text{SUSY}})} \tag{20}$$

where

$$g_{hbb} = \frac{g m_b}{2 m_W} \frac{\sin\alpha}{\cos\beta} = -\frac{g m_b}{2 m_W}(\sin(\beta-\alpha) - \tan\beta\cos(\beta-\alpha)) \tag{21}$$

$$g_{Hbb} = \frac{g m_b}{2 m_W} \frac{\cos\alpha}{\cos\beta} == \frac{g m_b}{2 m_W}(\cos(\beta-\alpha) + \tan\beta\sin(\beta-\alpha)) \tag{22}$$

$$g_{Abb} = \frac{g m_b}{2 m_W}\tan\beta \tag{23}$$

As we can see from the above equations, all Higgs couplings to the bottom quarks have some $\tan\beta$ enhancement at large $\tan\beta$ limit. Note also that an other $\tan\beta$ dependence comes through $\Delta_b$ corrections. We now have all the ingredients to compute the chargino and neutralino pair production at the LHC.

## III. PRODUCTION PROCESSES AND CONSTRAINTS

### A. $pp \to \tilde{\chi}_i \overline{\tilde{\chi}}_j$ via quark annihilation and gluon fusion

As stated early, the colorless fermionic superparticle pair production is through $gg \to \tilde{\chi}_i \overline{\tilde{\chi}}_j$ and $q\bar{q} \to \tilde{\chi}_i \overline{\tilde{\chi}}_j$ channels at hadron colliders. For gluon-gluon fusion, only loop effects are involved. In terms of type of loop, we classify the one-loop diagrams into three groups and sketch them in Fig. 1. They are (1) triangle diagrams [Figure 1 (*v1*) and (*v4*)], (2) box diagrams [Fig. 1 (*b1*)-Fig. 1 ($b_6$)], and (3) the diagrams with quartic vertices [Fig. 1 (*c1*)-Fig. 1 (*c3*)], where $F$ in the loop denotes the SM quarks, $\tilde{Q}$ is the possible squarks, $S$ stands for the scalar bosons ($h^0$, $H^0$, $A^0$) in the MSSM and $V$ represents the gauge bosons $Z$ and $\gamma$. We note that since the electromagnetic interactions are independent of the species of $\tilde{\chi}_i$, there exist only the interactions $\tilde{\chi}_i - \tilde{\chi}_i - \gamma$ ($i = 1, 2$). For quark-antiquark annihilation, the leading contributions to $\tilde{\chi}_i \overline{\tilde{\chi}}_j$ production are only from the effects of tree level. The associated Feynman diagrams are displayed in Fig. 2. For chargino-pair production, the squark $\tilde{u}_m$ in Fig. 2(c) could be up (down) type squark while the squark $\tilde{q}$ could be down (up) type squark. Although the gluon-gluon fusion loop, $s$-channel gauge boson exchange and $t$-channel squark exchange contributions have been studied in the literature, we emphasize that the effects of Fig. 2(a) with $q = b$ and large $\tan\beta$ on the $\tilde{\chi}_i \overline{\tilde{\chi}}_j$ production have not been explored yet. Moreover, since the masses of scalar bosons are free parameters, when the condition $(p_{\tilde{\chi}_i} + p_{\bar{\tilde{\chi}}_j})^2 \approx m^2_{H^0,A^0}$ is satisfied, the production cross section will be enhanced by the resonant Higgs effects.

By combining the contributions of gluon-gluon fusion and quark-antiquark annihilation, the cross section for $\tilde{\chi}_i \overline{\tilde{\chi}}_j$ production in proton-proton collisions at center-of-mass energy $\sqrt{s}$ can be written as

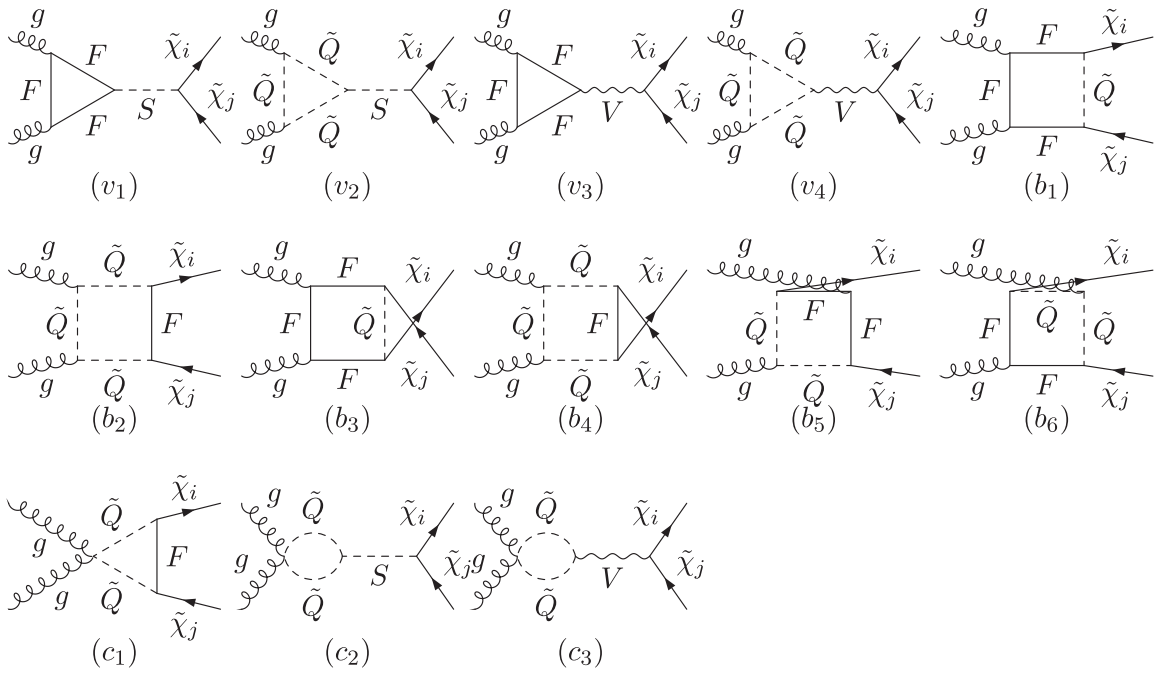


FIG. 1. One-loop Feynman diagrams of chargino-pair production at the LHC via gluon-gluon fusion with $S = h^0$, $H^0$ or $A^0$, $V = Z$ and $\gamma$ (only if $i = j$) and $\tilde{Q} = \tilde{u}$ or $\tilde{d}$ is squark.

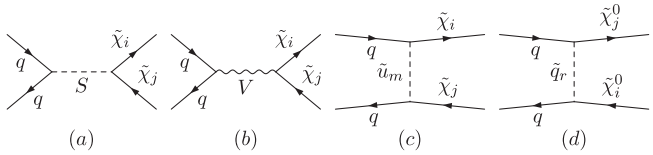


FIG. 2. Tree-level Feynman diagrams of chargino-pair production at the LHC via quark-anti-quark annihilation with $S = h^0$, $H^0$ or $A^0$, $V = Z$ and $\gamma$ (only if $i = j$) and $\tilde{u}_m$ is a squark corresponding to quark $q$.

$$\sigma_{\tilde{\chi}_i^+\tilde{\chi}_j^-}(s) = \sum_q \int_{\tau_0}^1 d\tau \frac{d\mathcal{L}_{q\bar{q}}^{pp}}{d\tau} \hat{\sigma}_{LO}(q\bar{q} \to \tilde{\chi}_i^+\tilde{\chi}_j^-)(\tau s) + \int_{\tau_0}^1 d\tau \frac{d\mathcal{L}_{gg}^{pp}}{d\tau} \hat{\sigma}_{LO}(gg \to \tilde{\chi}_i^+\tilde{\chi}_j^-)(\tau s) \quad (24)$$

with $\tau_0 = (m_{\tilde{\chi}_i}^2 + m_{\tilde{\chi}_j}^2)^2/s$, and the parton luminosity is

$$\frac{d\mathcal{L}_{ab}^{pp}}{d\tau} = \int_\tau^1 \frac{dx}{x} \frac{1}{1+\delta_{ab}} \left[ f_a(x,\mu_F) f_b\left(\frac{\tau}{x},\mu_F\right) + f_b(x,\mu_F) f_a\left(\frac{\tau}{x},\mu_F\right)\right] \quad (25)$$

where $f_a(x, \mu_F)$ is parton distribution function (PDF) for parton $a$ inside proton and $x$ is the momentum fraction at the scale $\mu_F = m_{\tilde{\chi}_i} + m_{\tilde{\chi}_j}$.

### B. Constraints on the free parameters of the MSSM

For studying the numerical analysis, we need the information of constraints that are from experimental conditions and data and theoretical requirements [33,34]. We summarize them as follows:

(i) The most stringent constraint generally arises from $\Delta\rho^{\rm SUSY}$ which receives contributions from both stop and sbottom. The extra contributions to the $\Delta\rho^{\rm SUSY}$ parameter from the stop and sbottom sector [35,36] should not exceed the current limit from precision measurements [37] i.e. $\Delta\rho^{\rm SUSY} \leq 10^{-3}$. Note that this constraint will not affect the parameter space that is associated with the effects of charginos and neutralinos [36].

(ii) The soft SUSY-breaking parameters $A_q$ at the weak scale should not be too large in order to keep the radiative corrections to the Higgs masses under control. In particular the trilinear couplings of the third generation squarks $A_{t,b}$, will play a particularly important role in the MSSM squarks/Higgs sectors. These parameters can be constrained in at least one way, besides the trivial requirement that it should not make the off-diagonal term of the squark mass matrices too large to generate too low masses for the squarks. $A_{t,b}$ should not be too large to avoid the occurrence of charge and color breaking (CCB) minima in the Higgs potential [38].

(iii) Another constraint is the perturbativity of the bottom Yukawa coupling $Y^b$. Since the radiative corrections to the bottom Yukawa couplings have been implemented in Eq. (17) that may blow up when SUSY parameters vary. Thus, we adopt $Y^b \lesssim (4\pi)^2$.

(iv) We have imposed also all the experimental bounds on squark, chargino, and neutralino masses as well as Higgs boson masses [37].

(v) We assume that $\tilde{\chi}_1^0$ is the LSP and will escape from the detection.

## IV. NUMERICAL ANALYSIS AND DISCUSSIONS

After introducing the physical effects and constraints, we now discuss the numerical analysis for the inclusive production cross sections of chargino and neutralino with $\sqrt{s} = 7$ and 14 TeV at the LHC. Since there are many free parameters in MSSM, for simplifying the study, we adopt the scenario of universal soft SUSY breaking for the trilinear couplings, i.e. $A_t = A_b$, and for the squark masses to be $M_{\tilde{Q}} = M_{\tilde{U}} \equiv M_{\rm SUSY}$. Accordingly, the Higgs masses $m_{h^0,H^0,H^\pm}$ and mixing $\alpha$ are fixed in terms of the $CP$-odd mass $m_{A^0}$, $\tan\beta$ as well as $M_{\rm SUSY}$, $A_{b,t}$, $M_2$ and $\mu$ for higher order corrections [39]. All the MSSM Higgs masses and relevant parameters are computed with FeynHiggs code [39]. We use CTEQ6L parton distribution functions [40,41] to estimate the various cross sections. Moreover, in order to improve the perturbative calculations, one-loop running mass formula for $m_b(Q)$ is taken by

$$m_b(Q) = m_b^{\overline{\rm DR}}(Q) = m_b^{\overline{\rm MS}}(Q)\left(1 + \frac{4\alpha_s}{3\pi}\right), \quad (26)$$

where $m_b^{\overline{\rm MS}}$ includes the SM QCD corrections and the running QCD coupling $\alpha_s$ is calculated at the two-loop level [42]. The light-quark masses are neglected in the numerical calculations. Other values of SM parameters are chosen as $m_t = 173$ GeV, $m_W = 80.398$ GeV, $m_Z = 91.1878$ GeV and $m_b(m_b) = 4.25$ GeV [37]. The fine structure constant is taken at the $Z$ pole with $\alpha_{ew}(m_Z^2) = 1/128$ [37]. For other MSSM parameters, we will perform a systematic scan in the following range:

(i) 120 GeV $\leq m_{A^0} \leq$ 600 GeV;

(ii) $3 \leq \tan\beta \leq 40$;

(iii) 100 GeV $\leq \mu \leq$ 1 TeV; The sign of $\mu$ is taken positive, as preferred by the SUSY explanation of the $(g-2)_\mu$ anomaly.

(iv) 100 GeV $\leq M_2 \leq$ 450 TeV; We impose the GUT relation at weak scale to fix $M_1$.

Before displaying our results, we emphasize that the MSSM parameter space has been subject to the experimental constraints of Tevatron and LHC by the negative

search of some specific processes. By looking to the Higgs boson production in tau-tau final states, both Tevatron and CMS [43,44] have set a limit on ($\tan\beta$, $m_{A^0}$) for some specific scenarios in the framework of the MSSM. From CDF and DØ (respectively CMS) data, those limits on ($\tan\beta$, $m_{A^0}$) are only valid for $m_{A^0} \lesssim 200$ GeV (respectively $m_{A^0}$300 GeV). From CMS data $\tan\beta \geq 30$ is already excluded for $100 \lesssim m_{A^0} \lesssim 200$ GeV in the MSSM with maximal mixing scenario, while for $200 \lesssim m_{A^0} \lesssim 300$ GeV the $\tan\beta$ is limited in the range [30, 55]. For our presentation, we will not restrict ourselves with those experimental constraints shown in Refs. [43,44] but rather present a complete scan over the MSSM parameter space. In the mean time, in our analysis we restrict ourselves to the $\tan\beta \lesssim 40$ for which $m_{A^0} \geq 150$ GeV is allowed. However, according to ATLAS and CMS analysis [43,44] care must be taken for low value of $m_{A^0} \approx 150$ GeV where $\tan\beta$ should be less than $\approx 25$.

In order to obtain the correct numerical results, we first check the calculations for chargino and neutralino pair production by gluon-gluon fusion in mSUGRA model. Our results are qualitatively consistent with Ref. [14,15]. For illustration, we show the production cross sections as a function of $\tan\beta$ [$m_{A^0}$] at $\sqrt{s} = 14$ TeV for $\sigma(b\bar{b}, gg, \sum q\bar{q} \to \tilde{\chi}_1^+ \tilde{\chi}_1^-)$ and $\sigma(b\bar{b}, gg, \sum q\bar{q} \to \tilde{\chi}_1^+ \tilde{\chi}_2^- + c.c)$ in Fig. 3(a), 3(b), 4(a), and 4(b), respectively. All the cross sections presented here are only at the leading order without K-factor. The NLO corrections to chargino/neutralino pair production have been done in Ref. [13], where the K-factor is taken by 1.25 (1.40) for $m_\chi \approx 250(100)$ GeV. In order to understand the sensitivities of $m_{A^0}$ and $\tan\beta$, in the figures we show separately the process for producing chargino pair, e.g., the curve of $b\bar{b}$ (no-Higgs) denotes the bottom-induced Drell-Yan contributions in which the processes include the $s$-channel photon and $Z$ boson exchange and $t$-channel with squark exchange. As to the curve of $b\bar{b}$, it stands for all Higgs-mediated effects and has the

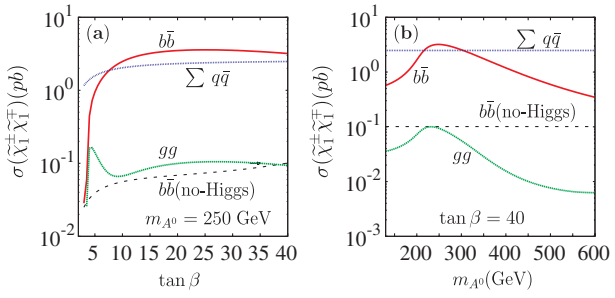


FIG. 3 (color online). Separate cross sections for chargino-pair production $\sigma(\tilde{\chi}_1^\pm \tilde{\chi}_1^\mp)(pb)$ in picobarn at the LHC with $\sqrt{s} =$ 14 TeV as a function of $\tan\beta$ (left) and $m_{A^0}$ (right). The SUSY parameters are chosen to be $M_{\rm SUSY} = 490$ GeV $M_2$, $\mu = 120$, 150 GeV, $A_t = A_b = 1140$ GeV.

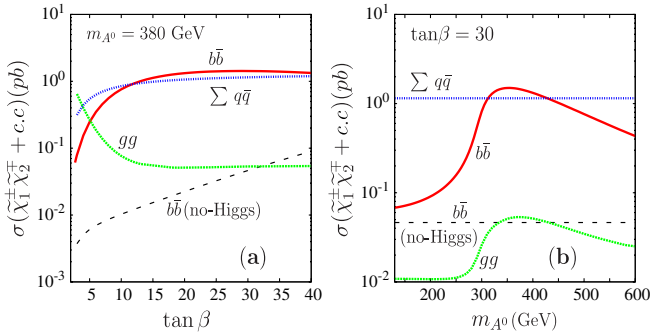


FIG. 4 (color online). Separate cross sections for chargino-pair production $\sigma(\tilde{\chi}_1^+ \tilde{\chi}_2^- + c.c)(pb)$ in picobarn at the LHC with $\sqrt{s} = 14$ TeV as a function of $\tan\beta$ (left) and $m_{A^0}$ (right). The SUSY parameters are chosen to be $M_2$, $\mu = 120$, 150 GeV, $A_t = A_b = 1140$ GeV.

enhancement of large $\tan\beta$ that we would like to emphasize in this paper.

Hence, from Figs. 3(a) and 4(a), it is easy to find that although at low $\tan\beta$ the production cross section is dominated by the light-quark fusion, however, the contributions from Higgs-mediated effects through $b\bar{b}$ annihilation will be over the light-quark fusion when $\tan\beta$ is around 10. The results show not only the sensitivity of production cross section to $\tan\beta$ but also the importance of $\tan\beta$ in the mechanism of Higgs exchange, i.e., the Higgs-mediated effects with large $\tan\beta$ could become dominant in chargino-pair production. Beside the $\tan\beta$ enhanced factor, as mentioned earlier, Higgs-resonance can be another effect to enhance the chargino-pair production. We can see the enhancement from Figs. 3(b) and 4(b). By the curve arisen from $b\bar{b}$ fusion, it is clear that there is a bump at $m_{A^0} \approx 250[350]$ GeV in Fig. 3(b) and 4(b), where the bump is formed when $m_{H^0} \approx m_{A^0} \approx 2m_{\tilde{\chi}_1^+}$ is satisfied. We note that the curve denoted by $b\bar{b}$ (no-Higgs) is not sensitive to $\tan\beta$ and has no Higgs-resonance, therefore, its contribution is far below that by Higgs-mediated effects. Although gluon-gluon fusion can contribute to chargino-pair production by loop effects, its contributions are much smaller than those from $q\bar{q}$ and $b\bar{b}$ fusion, except the case for $gg \to \tilde{\chi}_1^\pm \tilde{\chi}_2^\mp$ at low $\tan\beta$. Since we are considering the scenario with large $\tan\beta$, gluon-gluon fusion is not a dominant process. Therefore, we do not further discuss the gluon-gluon fusion in detail.

Next, we discuss the situation for neutralino-pair production. Since the lightest neutralino-pair is associated with invisible signal, we skip the relevant discussions. Accordingly, we will concentrate on the production of $\chi_1^0 \chi_2^0$ and $\chi_2^0 \chi_2^0$ pairs. Additionally, the production channels $pp \to \tilde{\chi}_1^0 \tilde{\chi}_2^0$ and $pp \to \tilde{\chi}_2^0 \tilde{\chi}_2^0$ are of special interest because of the presence of dileptons in their decay products.

Similar to the chargino cases, we show various production cross section $\sigma(b\bar{b}, gg, \sum q\bar{q} \to \tilde{\chi}_1^0 \tilde{\chi}_2^0, \tilde{\chi}_2^0 \tilde{\chi}_2^0)$ as a

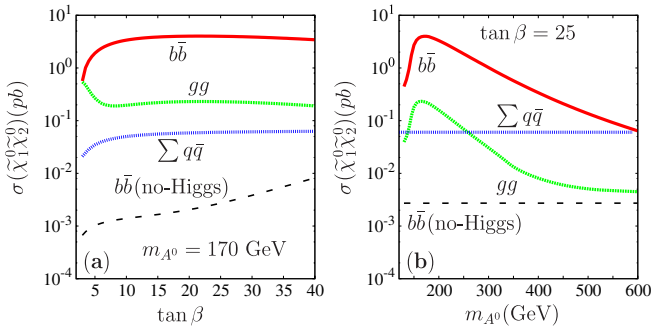


FIG. 5 (color online). Separate cross sections for neutralino-pair production $\sigma(\tilde{\chi}_1^0\tilde{\chi}_2^0)(pb)$ at the LHC with $\sqrt{s} = 14$ TeV as a function of $\tan\beta$ (left) and as a function of $m_{A^0}$ (right). The SUSY parameters are chosen to be $M_{\rm SUSY} = 490$ GeV, $M_2 = 120$ GeV, $\mu = 150$ GeV and $A_t = A_b = 1140$ GeV.

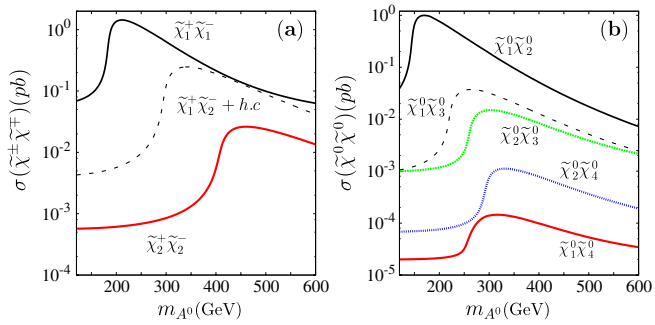


FIG. 7 (color online). Total cross sections for chargino (left) and neutralino (right) pairs production at the LHC with $\sqrt{s} = 7$ TeV as a function of $m_{A^0}$. The SUSY parameters are chosen to be $M_{\rm SUSY} = 490$ GeV, $M_2 = 120$ GeV, $M_{\rm SUSY} = 490$ GeV, $\mu = 150$ GeV, $A_t = A_b = 1140$ GeV and is fixed at $\tan\beta = 20$.

function of $\tan\beta$ [$m_{A^0}$] in Fig. 5 and 6 for 14 TeV LHC energy. In both cases, near the resonance region and for large $\tan\beta$, one can see that $b\bar{b}$ fusion contribution is more important than $q\bar{q}$ contribution and can go up to 1 order of magnitude larger exceeding few picobarn in some cases. This is mainly due to the smallness of $Z\tilde{\chi}_i^0\tilde{\chi}_j^0$ coupling which contributes to $q\bar{q}$ fusion through $Z$ exchange. Moreover, in the mixed ($|\mu| \sim M_2$) regime, the first and second generation squarks would be significantly heavier than wino like charginos and neutralinos, making the $t$-channel contribution negligible with respect to the $s$-channel contribution which enjoy the resonant effect $\sqrt{\hat{s}} \approx m_{H^0,A^0} \approx 2m_{\tilde{\chi}}$. It has to be noted also that the gluon-gluon fusion $gg \to \tilde{\chi}_i^0\tilde{\chi}_j^0$, both for diagonal production $\tilde{\chi}_2^0\tilde{\chi}_2^0$ as well as for nondiagonal one $\tilde{\chi}_1^0\tilde{\chi}_2^0$, is in some cases larger that the $q\bar{q}$ fusion in the case of low $\tan\beta$.

For comparison, we also present the results for the production of chargino and neutralino at $\sqrt{s} = 7$ TeV in Fig. (7). It is easy to see that large $\tan\beta$ and the Higgs resonant effects could also enhance the cross sections of $\tilde{\chi}_i^+\tilde{\chi}_j^-$ and $\tilde{\chi}_i^0\tilde{\chi}_j^0$ by about 1 order of magnitude and the cross sections for the production of $\tilde{\chi}_1^+\tilde{\chi}_1^-$ and $\tilde{\chi}_1^0\tilde{\chi}_2^0$ could be up to 1 pb. In addition, we also investigate the processes that chargino and neutralino are in the final state, e.g. $pp \to \tilde{\chi}_i^0\tilde{\chi}_j^\pm$. The production mechanism proceeds via the conventional Drell-Yan processes with W gauge boson, charged Higgs boson and charged Goldstone. The dominant contribution is through $W$ gauge boson exchange. The charged Higgs contribution is through $c\bar{b} \to H^{\pm *} \to \tilde{\chi}_i^+\tilde{\chi}_j^0$ and the enhancement of large $\tan\beta$ is from the bottom Yukawa coupling. Unfortunately, it turns out that this large $\tan\beta$ enhancement can not overcome the suppression from $V_{cb}$ Cabibbo-Kobayashi-Maskawa (CKM) matrix element.

To quantify those effects from $s$-channel Higgs exchange contribution and to show their importance, we provide some scatter plots in ($\mu$, $M_2$) and ($\tan\beta$, $m_{A^0}$) plans. From the results in Figs. 8(a) and 9(a), we see that

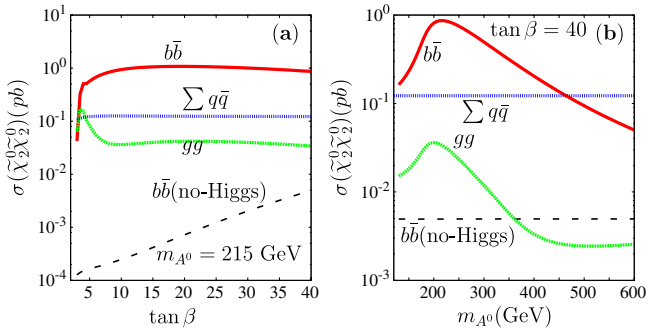


FIG. 6 (color online). Separate cross sections for neutralino-pair production $\sigma(\tilde{\chi}_2^0\tilde{\chi}_2^0)(pb)$ at the LHC with $\sqrt{s} = 14$ TeV as a function of $\tan\beta$ (left) and as a function of $m_{A^0}$ (right). The SUSY parameters are chosen to be $M_{\rm SUSY} = 490$ GeV, $M_2 = 120$ GeV, $m_{\tilde{g}} = 1$ TeV, $\mu = 150$ GeV, $A_t = A_b = 1140$ GeV.

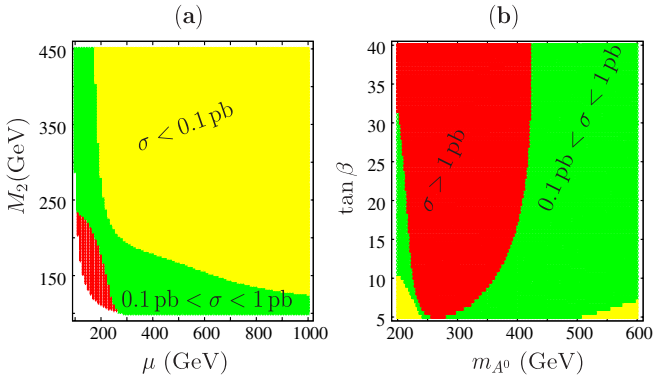


FIG. 8 (color online). Scatter plots of $\sigma(pp \to b\bar{b} \to \tilde{\chi}_1^-\tilde{\chi}_1^+)$ in the ($\mu$, $M_2$) plan (left) and ($m_{A^0}$, $\tan\beta$) plan (right). The SUSY parameters are chosen to be $M_{\rm SUSY} = 490$ GeV, $A_t = A_b = 1140$ GeV, ($m_{A^0} = 350$ GeV, $\tan\beta = 20$) and ($M_2 = \mu = 150$ GeV) for left and right panels, respectively.

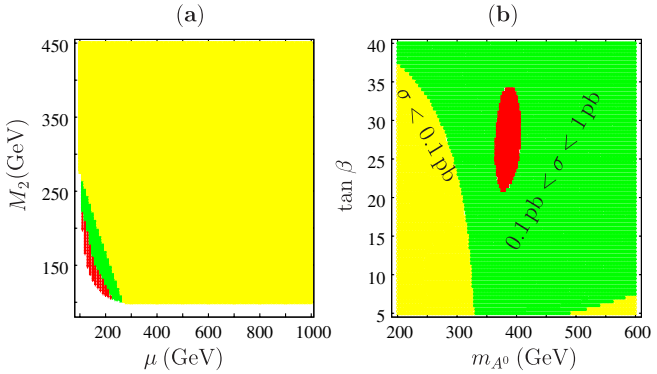


FIG. 9 (color online). Scatter plots of $\sigma(pp \to b\bar{b} \to \tilde{\chi}_1^- \tilde{\chi}_2^+ + c.c)$ in the $(\mu, M_2)$ plan (left) and $(m_{A^0}, \tan\beta)$ plan (right). The other parameters are fixed as in Fig. (8).

with $\mu \lesssim 250$ GeV and $M_2 \lesssim 250$ GeV, since we are very close to the resonant region, the cross section is slightly larger than 1 pb. In the case of diagonal production of $\tilde{\chi}_1^+ \tilde{\chi}_1^-$, the region with large $\mu$ and moderate $M_2$ (gaugino-like), or large $M_2$ and moderate $\mu$ (higgsino-like) is interesting (see Fig. 8(a)). This is because the process is dominated by the $s$-channel $Z^0$ exchange and the cross section can be in the range 0.1–1 pb. Because of the phase space suppression, nondiagonal production $\tilde{\chi}_1^+ \tilde{\chi}_2^-$ will be small in this region. On the other hand we show in Fig. 8(b) and 9(b) the production cross section in the plan ( $\tan\beta, m_{A^0}$. Here we can see the resonant effect for $\tilde{\chi}_1^+ \tilde{\chi}_1^-$ when $m_{A^0} \approx m_{H^0} \approx 280$ GeV. This effect is amplified for large $\tan\beta$. There is also a large area where the diagonal production cross section $\tilde{\chi}_1^+ \tilde{\chi}_1^-$ is in the range 0.1–1 pb. In the case of nondiagonal production $\tilde{\chi}_1^+ \tilde{\chi}_2^-$ and due to phase space suppression the resonance effect is rather mild. That is the reason why one can see only small region for $\tan\beta \in [20, 35]$ where the cross section is larger than 1 pb.

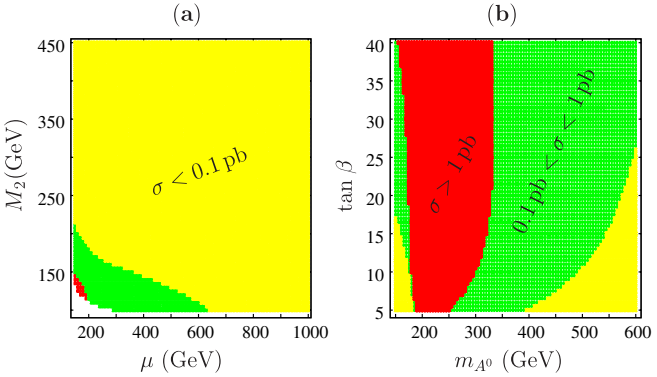


FIG. 10 (color online). Scatter plots of $\sigma(pp \to b\bar{b} \to \tilde{\chi}_1^0 \tilde{\chi}_2^0)$ in the $(\mu, M_2)$ plan (left) and $(m_{A^0}, \tan\beta)$ plan (right). The SUSY parameters are chosen to be $(m_{A^0} = 220$ GeV, $\tan\beta = 20)$ and $(M_2 = 120$ GeV, $\mu = 150$ GeV) for left and right panels, respectively.

TABLE I. The effect of the $s$-channel Higgs ($H^0$, $A^0$) on the production cross sections (in pb). The SUSY parameters are chosen to be $A_t = A_b = 1140$ GeV, $\mu = 150$ GeV, $M_2 = 120$ GeV, $M_{\rm SUSY} = 490$ GeV, $m_{\tilde{g}} = 1$ TeV, $\tan\beta = 40$ and the Higgs masses are taken at the resonance.

| | $\sqrt{s} = 14$ TeV | | $\sqrt{s} = 7$ TeV | |
|---|---|---|---|---|
| $\sigma$ [pb] | Higgs Only | Full | Higgs Only | Full |
| $b\bar{b} \to \tilde{\chi}_1^+ \tilde{\chi}_1^-$ | 3.761 | 3.881 | 0.727 | 0.755 |
| $b\bar{b} \to \tilde{\chi}_1^+ \tilde{\chi}_2^-$ + H.c. | 0.498 | 0.504 | 0.072 | 0.074 |
| $b\bar{b} \to \tilde{\chi}_2^+ \tilde{\chi}_2^-$ | 0.054 | 0.066 | 0.006 | 0.007 |
| $gg \to \tilde{\chi}_1^+ \tilde{\chi}_1^-$ | 0.134 | 0.149 | 0.122 | 0.006 |
| $gg \to \tilde{\chi}_1^+ \tilde{\chi}_2^-$ + H.c. | 0.086 | 0.098 | 0.081 | 0.019 |
| $gg \to \tilde{\chi}_2^+ \tilde{\chi}_2^-$ | 0.043 | 0.015 | 0.001 | 0.002 |
| $b\bar{b} \to \tilde{\chi}_1^0 \tilde{\chi}_2^0$ | 2.822 | 2.750 | 0.645 | 0.630 |
| $b\bar{b} \to \tilde{\chi}_2^0 \tilde{\chi}_2^0$ | 1.384 | 1.333 | 0.285 | 0.276 |
| $gg \to \tilde{\chi}_1^0 \tilde{\chi}_2^0$ | 0.805 | 0.789 | 0.241 | 0.205 |
| $gg \to \tilde{\chi}_2^0 \tilde{\chi}_2^0$ | 0.301 | 0.272 | 0.071 | 0.064 |

In the case of the associate production $\tilde{\chi}_1^0 \tilde{\chi}_2^0$ we show the scatter plots in Fig. 10 in $(\mu, M_2)$ and $(m_{A^0}, \tan\beta)$ plans. When $|\mu| \gg M_2$ the two lightest neutralinos are both nearly pure gauginos, their $s$-channel contribution is then small, the squarks exchange diagrams play the most important role in this case. Unlike $\tilde{\chi}_1^+ \tilde{\chi}_2^-$ which suffers phase space suppression, $\tilde{\chi}_1^0 \tilde{\chi}_2^0$ does not have such suppression. This is mainly due to the fact that $m_{\chi_2^0} \approx m_{\chi_1^\pm}$ (see section B 1). Therefore, we can see in Fig. 10(b) the same resonance effect we have seen in the case of $\tilde{\chi}_1^+ \tilde{\chi}_1^-$.

Finally, in Table I we give separate contributions to $b\bar{b}$ and gluon-gluon fusion that originate from $s$-channel of Higgs $A^0$ and $H^0$ exchange only and also from the full set of Feynman diagrams. It is clear from this table that $s$-channel Higgs exchange contribution is the dominant one. This can be viewed as a production of the Heavy Higgs bosons followed by the subsequent decays into a chargino or neutalino pairs [18,19].

## V. CONCLUSION

We have studied the pair production of charginos and neutralinos in detail where the study includes the tree level $s$-channel Higgs bosons exchange and the radiative corrections to the bottom Yukawa couplings. It has been shown that the $s$-channel Higgs bosons effect can enhance substantially the production cross section in the mixed region when $M_2$ and $|\mu|$ are comparable and below 1 TeV. Such enhancement can go up to 1 order of magnitude compared to the usual $q\bar{q}$ fusion contribution. We have demonstrated that the enhancement has two origins: on one hand the large $\tan\beta$ enhancement and on the other hand resonance effect from $s$-channel Higgs bosons. Such enhancements exceed the PDF uncertainties

on the evaluation of the cross section and are in some case larger than the NLO correction. Therefore, these contributions have to be taken into account in any reliable future analysis. We have found that in the low $\tan\beta$ regime, the gluon fusion contribution could be comparable to $q\bar{q}$ and $b\bar{b}$ one. Those processes can be used to extract some information on the chargino and neutralino Higgs couplings right at the Higgs boson resonances and the involved SUSY parameters.

## ACKNOWLEDGMENTS

We thank Federico von der Pahlen for helpful discussions. A. A is supported by the NSC under Contract No. 100-2811-M-006-008. The work of R. B was supported by CSIC. M. C. would like to thank C-H. Chen and H-N. Li for their invitation and hospitality at NCKU and Academia Sinica and acknowledge NCTS support. CHC was supported by NSC Grant No. NSC-97-2112-M-006-001-MY3.

## APPENDIX A: SUSY COUPLINGS

We describe in this appendix all the couplings of these SUSY particles i.e. couplings of the neutralinos and charginos to gauge and Higgs bosons and their couplings to fermion-sfermion pairs as well as the couplings of MSSM Higgs and gauge bosons to fermions, which will be needed later when evaluating the cross sections of $2 \to 2$ processes. We will use the notation of [12,24].

### Chargino and Neutralino Interactions

We start this section by discussing the chargino and neutralino interactions with gauge bosons ($\gamma$, $Z$ and $W^{\pm}$), Higgs bosons as well as fermion-sfermions pairs. The resulting charged and neutral weak boson terms in the Lagrangian density, expressed in the four component notation and in the weak basis reads

$$\begin{aligned}\mathcal{L} = & -eA_\mu \overline{\tilde{\chi}_k^+}\gamma^\mu \tilde{\chi}_k^+ + \frac{g}{c_W} Z_\mu \sum_{\alpha,m,k} \overline{\tilde{\chi}_m^+}\,\gamma^\mu \mathcal{O}_{mk}^{\alpha} P_\alpha \tilde{\chi}_k^+ \\ & + \frac{g}{2c_W} Z_\mu \sum_{\alpha,l,n} \overline{\tilde{\chi}_l^0}\,\gamma^\mu \mathcal{N}_{ln}^{\alpha} P_\alpha \tilde{\chi}_n^0 \\ & + \left[ g W_\mu^- \sum_{\alpha,l,k} \overline{\tilde{\chi}_l^0}\,\gamma^\mu \mathcal{C}_{lk}^{\alpha} P_\alpha \tilde{\chi}_k^+ + \text{H.m} \right] \end{aligned} \tag{A1}$$

where $g = e/s_W$, $k$, $m = 1,2$ for the chargino and $l$, $n = 1,\ldots 4$ for the neutralino, $\alpha = L$, $R$ with $P_{L,R} = (1 \mp \gamma_5)/2$. The couplings $\mathcal{O}_{mk}^{\alpha}$, $\mathcal{N}_{ln}^{\alpha}$ and $\mathcal{C}_{lk}^{\alpha}$ are given by

$$\mathcal{O}_{mk}^{L} = -V_{m1} V_{k1}^* - \frac{1}{2} V_{m2} V_{k2}^* + \delta_{mk} s_W^2, \tag{A2}$$

$$\mathcal{O}_{mk}^{R} = -U_{m1}^* U_{k1} - \frac{1}{2} U_{m2}^* U_{k2} + \delta_{mk} s_W^2, \tag{A3}$$

$$\mathcal{N}_{ln}^{L} = -\frac{1}{2} Z_{l3} Z_{n3}^* + \frac{1}{2} Z_{l4} Z_{n4}^*, \tag{A4}$$

$$\mathcal{N}_{ln}^{R} = -(\mathcal{N}_{ln}^{L})^*, \tag{A5}$$

$$\mathcal{C}_{lk}^{L} = -\frac{1}{\sqrt{2}} Z_{l4} V_{k2}^* + Z_{l2} V_{k1}^*, \tag{A6}$$

$$\mathcal{C}_{lk}^{R} = \frac{1}{\sqrt{2}} Z_{l3}^* U_{k2} + Z_{l2}^* U_{k1}. \tag{A7}$$

$Z$, $U$, $V$ are the neutralino and chargino mixing matrices, respectively. The unitarity properties of the $U$ and $V$ matrices have been used in deriving Eqs. (A2)–(A7).

The couplings of the Higgs bosons to the electroweak neutralinos and charginos originate from the gauge strength Yukawa couplings of gauginos to the scalar and fermionic components of a given chiral supermultiplet. In four-conponent the Lagrangian reads as:

$$\begin{aligned}\mathcal{L} = & -\frac{g}{2} \sum_{i=1,2} H_i^0 \overline{\tilde{\chi}_l^0} S_{lni} \tilde{\chi}_n^0 - \frac{g}{2} \sum_{i=3,4} H_i^0 \overline{\tilde{\chi}_l^0} S_{lni} \gamma_5 \tilde{\chi}_n^0 \\ & - g \sum_{i=1,2} H_i^0 \overline{\tilde{\chi}_k^+} (C_{kmi} P_R + C_{mki}^* P_L) \tilde{\chi}_m^+ \\ & + ig \sum_{i=3,4} H_i^0 \overline{\tilde{\chi}_k^+} (C_{kmi} P_R + C_{mki}^* P_L) \tilde{\chi}_m^+ \\ & - g \sum_{i=1,2} [H_i^+ \overline{\tilde{\chi}_k^+} (F_{kli}^R P_R + F_{kli}^L P_L) \tilde{\chi}_l^0 + \text{H.c}] \end{aligned} \tag{A8}$$

where the couplings are given by:

$$\begin{aligned} S_{lni} = & \frac{e_i}{2} [Z_{l3} Z_{n2} + Z_{n3} Z_{l2} - \tan\theta_W (Z_{l3} Z_{n1} + Z_{n3} Z_{l1})] \\ & + \frac{d_i}{2} [Z_{l4} Z_{n2} + Z_{n4} Z_{l2} - \tan\theta_W (Z_{l4} Z_{n1} + Z_{n4} Z_{l1})], \end{aligned} \tag{A9}$$

$$C_{kmi} = \frac{1}{\sqrt{2}} (e_i V_{k1} U_{m2} - d_i V_{k2} U_{m1}) \tag{A10}$$

$$C_{mki}^* = C_{kmi} \ \text{ for } i = 1,2 \ \text{ and } \ C_{mki}^* = -C_{kmi} \ \text{ for } i = 3,4 \tag{A11}$$

$$F^R_{kli} = d_{i+2}[V_{k1}Z_{l4} + \frac{1}{\sqrt{2}}(Z_{l2} + Z_{l1}\tan\theta_W)V_{k2}] \quad \text{(A12)}$$

$$F^L_{kli} = -e_{i+2}[U_{k1}Z_{l3} - \frac{1}{\sqrt{2}}(Z_{l2} + Z_{l1}\tan\theta_W)U_{k2}] \quad \text{(A13)}$$

Again, here we have used $k, m = 1, 2$ for the chargino and $l,\ n = 1, \ldots 4$ for the neutralino. $H^0_i = (h^0, H^0, A^0, G^0)$ $(i = 1 \ldots 4)$, and $H^+_i = (H^+, G^+)$ $(i = 1,\ 2)$ $d_i$ and $e_i$ take the values

$$\begin{aligned} d_i &= (-\cos\alpha, -\sin\alpha, \cos\beta, \sin\beta), \\ e_i &= (-\sin\alpha, \cos\alpha, -\sin\beta, \cos\beta) \end{aligned} \quad \text{(A14)}$$

The squark-quark-chargino Lagrangian is given by,

$$\begin{aligned} \mathcal{L} = g[&\bar{u}A^L_{sk}P_R\tilde{d}_s\tilde{\chi}^+_k + \tilde{d}^\dagger_s\overline{\tilde{\chi}^+_k}B^L_{sk}P_R u + \bar{d}E^R_{sk}P_R\tilde{u}_s(\tilde{\chi}^+_k)^C \\ &+ \tilde{u}^\dagger_s(\tilde{\chi}^+_k)^C F^L_{sk}P_L d] + \text{H.c} \end{aligned} \quad \text{(A15)}$$

with the following couplings

$$A^L_{sk} = -V_{ud}\left[U^*_{k1}R^{\tilde{d}}_{s1} - \frac{m_d}{\sqrt{2}M_W c_\beta}U^*_{k2}R^{\tilde{d}}_{s2}\right] \quad \text{(A16)}$$

$$B^L_{sk} = \frac{m_u}{\sqrt{2}M_W s_\beta}V_{k2}R^{\tilde{d}}_{s1}V_{ud} \quad \text{(A17)}$$

$$E^R_{sk} = -V_{ud}\left[V^*_{k2}R^{\tilde{u}}_{s2} - \frac{m_u}{\sqrt{2}M_W s_\beta}V^*_{k1}R^{\tilde{u}}_{s1}\right] \quad \text{(A18)}$$

$$F^L_{sk} = \frac{m_d}{\sqrt{2}M_W c_\beta}U^*_{k2}R^{\tilde{u}}_{s1}V_{ud} \quad \text{(A19)}$$

$R^{\tilde{d},\tilde{u}}_{ss'}$ with $(s,\ s' = 1,\ 2)$ are the elements of the rotation matrices diagonalizing the up- and down- type squark mass matrices, and $V_{ud}$ are the elements of the CKM matrix. The squark-quark-neutralino interaction can be written down in a similar way,

$$\begin{aligned} \mathcal{L} = g\overline{\tilde{\chi}^0_l}[&(G^{uL}_{isl}P_L + G^{uR}_{isl}P_R)\tilde{u}^\dagger_s u_i + (G^{dL}_{isl}P_L \\ &+ G^{dR}_{isl}P_R)\tilde{d}^\dagger_s d_i] + \text{H.c} \end{aligned} \quad \text{(A20)}$$

where the couplings are defined as

$$G^{uL}_{sl} = \sqrt{2}e_u\tan\theta_W R^{\tilde{u}}_{s2}Z^*_{n1} - \frac{m_u}{\sqrt{2}M_W s_\beta}R^{\tilde{u}}_{s1}Z^*_{n4} \quad \text{(A21)}$$

$$G^{uR}_{sl} = -\frac{m_u}{\sqrt{2}M_W s_\beta}R^{\tilde{u}}_{s2}Z_{n4} - \frac{e_u(s_W Z_{n1} + 3c_W Z_{n2})}{2\sqrt{2}c_W}R^{\tilde{u}}_{s1} \quad \text{(A22)}$$

$$G^{dL}_{sl} = \sqrt{2}e_d\tan\theta_W R^{\tilde{d}}_{s2}Z^*_{n1} - \frac{m_d}{\sqrt{2}M_W c_\beta}R^{\tilde{d}}_{s1}Z^*_{n3} \quad \text{(A23)}$$

$$G^{dR}_{sl} = -\frac{m_d}{\sqrt{2}M_W c_\beta}R^{\tilde{d}}_{s2}Z_{n3} + \frac{e_d(s_W Z_{n1} - 3c_W Z_{n2})}{2\sqrt{2}c_W}R^{\tilde{d}}_{s1} \quad \text{(A24)}$$

with $e_u = 2/3$ and $e_d = -1/3$.

## APPENDIX B: PRODUCTION RATES

The production of chargino/neutralino pair, as initiated by $b\bar{b}$ annihilation, involves photon, $Z$ and Higgs bosons in the $s$-channel as well as squark/slepton exchanges in the $t/u$-channels. We present the differential cross section for each subprocess separately in the mass eigen-basis. The summation and average of spin/color for final and initial states are taken into account. In the formulas presented below, summation over repeated indices $k$ and $k'$ for the Higgs bosons and $s$ and $l$ for the squark and sleptons in the intermediate states are understood. Now let us define our notation for the convenience of the following formulas. The momenta of the incoming quark $b$ and antiquark $\bar{b}$, outgoing $\tilde{\chi}_i$, and outgoing $\tilde{\chi}_j$ are denoted by $p_1$, $p_2$, $k_1$ and $k_2$, respectively. We neglect the quark masses of the incoming partons. The Mandelstam variables are defined as follows:

$$\begin{aligned} \hat{s} &= (p_1 + p_2)^2 = (k_1 + k_2)^2 \\ \hat{t} &= (p_1 - k_1)^2 = (p_2 - k_2)^2 \\ &= \frac{m^2_{\tilde{\chi}_i} + m^2_{\tilde{\chi}_j}}{2} - \frac{\hat{s}}{2}(1 - \beta\cos\theta^*) \\ \hat{u} &= (p_1 - k_2)^2 = (p_2 - k_1)^2 \\ &= \frac{m^2_{\tilde{\chi}_i} + m^2_{\tilde{\chi}_j}}{2} - \frac{\hat{s}}{2}(1 + \beta\cos\theta^*) \end{aligned} \quad \text{(B1)}$$

where $\beta = \lambda^{1/2}(1, m^2_{\tilde{\chi}_i}/\hat{s}, m^2_{\tilde{\chi}_j}/\hat{s})$ and $\theta^*$ is the scattering angle in the center-of-mass frame of the partons.

### 1. Chargino-pairs production

$$\frac{d\hat{\sigma}_{LO}}{d\hat{t}}(\tilde{\chi}_i^+\tilde{\chi}_j^-)=\frac{4\pi^2\alpha^2}{3s_W^4}\Big[\Big(\frac{8e_q^2}{\hat{s}^2}[\hat{s}^2+2(m^4_{\tilde{\chi}_i^\pm}-2m^2_{\tilde{\chi}_i^\pm}\hat{t}+\hat{s}\hat{t}+\hat{t}^2)]-\frac{4s_W^2e_q}{c_W}\frac{D_Z}{\hat{s}}[g_{RZ}(\hat{t}^2+m^4_{\tilde{\chi}_i^\pm}-2m^2_{\tilde{\chi}_i^\pm}\hat{t}-m^2_{\tilde{\chi}_i^\pm}\hat{s})(\mathcal{O}^L_{ij}+\mathcal{O}^R_{ij})$$
$$+\mathcal{O}^R_{ij}(\hat{s}^2+2\hat{s}\hat{t})+(L\leftrightarrow R)]+4\sqrt{2}e_qs_W^2\frac{D_\phi}{\hat{s}}C_{iik}g_{bb\phi}m_bm_{\tilde{\chi}_i^\pm}(\hat{s}+2\hat{t}-2m^2_{\tilde{\chi}_i^\pm})-\frac{e_qs_W^2}{\hat{s}}((E^R_{si})^2+(F^L_{si})^2)$$
$$\times[m^4_{\tilde{\chi}_i^\pm}+(\hat{s}+\hat{t})^2-m^2_{\tilde{\chi}_j^\pm}(\hat{s}+2\hat{t})]U_{\tilde{t}_s}\Big)\delta_{ij}+\frac{D_Z^2}{c_W^2}[g^2_{RZ}(2m_{\tilde{\chi}_i^\pm}m_{\tilde{\chi}_j^\pm}\mathcal{O}^L_{ij}\mathcal{O}^R_{ij}\hat{s}+(\mathcal{O}^L_{ij})^2\hat{s}^2+((\mathcal{O}^L_{ij})^2+(\mathcal{O}^R_{ij})^2)\hat{t}^2$$
$$+2(\mathcal{O}^L_{ij})^2\hat{s}\hat{t}+m^2_{\tilde{\chi}_i^\pm}[m_{\tilde{\chi}_j^\pm}((\mathcal{O}^L_{ij})^2+(\mathcal{O}^R_{ij})^2)-(\mathcal{O}^R_{ij})^2\hat{t}-(\mathcal{O}^L_{ij})^2(\hat{s}+\hat{t})]-m^2_{\tilde{\chi}_j^\pm}((\mathcal{O}^R_{ij})^2\hat{t}+(\mathcal{O}^L_{ij})^2(\hat{t}+\hat{s})))$$
$$+(L\leftrightarrow R)]+g^2_{bb\phi}D^2_\phi\hat{s}[(C^2_{ij\phi}+C^2_{ji\phi})(\hat{s}-m^2_{\tilde{\chi}_i^\pm}-m^2_{\tilde{\chi}_j^\pm})-4m_{\tilde{\chi}_i^\pm}m_{\tilde{\chi}_j^\pm}C_{ij\phi}C_{ji\phi}]+g^2_{bbA}D^2_A\hat{s}[(C^2_{ijA}+C^2_{jiA})$$
$$\times(\hat{s}-m^2_{\tilde{\chi}_i^\pm}-m^2_{\tilde{\chi}_j^\pm})+4m_{\tilde{\chi}_i^\pm}m_{\tilde{\chi}_j^\pm}C_{ijA}C_{jiA}]+((E^R_{si})^2+(F^L_{si})^2)((E^R_{sj})^2+(F^L_{sj})^2)\times(\hat{t}-m^2_{\tilde{\chi}_i^\pm})(\hat{t}-m^2_{\tilde{\chi}_j^\pm})T^2_{\tilde{t}_s}$$
$$+\frac{\sqrt{2}}{c_w}g_{bb\phi}D_\phi D_Zm_b(\hat{s}+2\hat{t}-m^2_{\tilde{\chi}_i^\pm}-m^2_{\tilde{\chi}_i^\pm})\times[(m_{\tilde{\chi}_i^\pm}C_{ji\phi}+m_{\tilde{\chi}_j^\pm}C_{ij\phi})\mathcal{O}^L_{ij}+(m_{\tilde{\chi}_i^\pm}C_{ij\phi}+m_{\tilde{\chi}_j^\pm}C_{ji\phi})\mathcal{O}^R_{ij}]$$
$$-\frac{\hat{s}m_b}{\sqrt{2}c_W^2M_Z^2}g_{bbA}D_AD_Z[(m^2_{\tilde{\chi}_i^\pm}-m^2_{\tilde{\chi}_j^\pm})(C_{ijA}(m_{\tilde{\chi}_j^\pm}\mathcal{O}^L_{ij}+m_{\tilde{\chi}_i^\pm}\mathcal{O}^R_{ij})-C_{jiA}(m_{\tilde{\chi}_i^\pm}\mathcal{O}^L_{ij}+m_{\tilde{\chi}_j^\pm}\mathcal{O}^R_{ij}))$$
$$+\hat{s}(C_{jiA}(m_{\tilde{\chi}_i^\pm}\mathcal{O}^L_{ij}-m_{\tilde{\chi}_j^\pm}\mathcal{O}^R_{ij})+C_{ijA}(m_{\tilde{\chi}_j^\pm}\mathcal{O}^L_{ij}-m_{\tilde{\chi}_i^\pm}\mathcal{O}^R_{ij}))]-\frac{2}{c_W}D_ZT_{\tilde{t}_s}[m_{\tilde{\chi}_i^\pm}m_{\tilde{\chi}_j^\pm}(F^L_{si}F^L_{sj}g_{RZ}$$
$$\times(m_{\tilde{\chi}_i^\pm}m_{\tilde{\chi}_j^\pm}\mathcal{O}^R_{ij}+\hat{s}\mathcal{O}^L_{ij})+E^R_{si}E^R_{sj}g_{LZ}(m_{\tilde{\chi}_i^\pm}m_{\tilde{\chi}_j^\pm}\mathcal{O}^L_{ij}+\hat{s}\mathcal{O}^R_{ij})-(\hat{t}-m^2_{\tilde{\chi}_i^\pm}-m^2_{\tilde{\chi}})E^R_{si}E^R_{sj}g_{LZ}\mathcal{O}^L_{ij}+F^L_{si}F^L_{sj}g_{RZ}\mathcal{O}^R_{ij})\hat{t}$$
$$+2g_{bbh}g_{bbH}\hat{s}D_hD_H[2m_{\tilde{\chi}_i^\pm}m_{\tilde{\chi}_j^\pm}(C_{ijh}C_{jiH}+C_{ijH}C_{jih})+(m^2_{\tilde{\chi}_i^\pm}+m^2_{\tilde{\chi}_j^\pm}-\hat{s})(C_{ijh}C_{ijH}+C_{jih}C_{jiH})$$
$$-\sqrt{2}g_{bb\phi}D_\phi T_{\tilde{t}_s}(C_{ij\phi}E^R_{sj}F^L_{si}+C_{jih}E^R_{si}F^L_{sj})(m_{\tilde{\chi}_i^\pm}m_{\tilde{\chi}_j^\pm}+\hat{t})\hat{t}$$
$$+2(E^R_{si}E^R_{s'i}+F^L_{si}F^L_{s'i})(E^R_{sj}E^R_{s'j}+F^L_{sj}F^L_{s'j})(\hat{t}-m^2_{\tilde{\chi}_i^\pm})(\hat{t}-m^2_{\tilde{\chi}_j^\pm})T_{\tilde{t}_s}T_{\tilde{t}_{s'}}\Big] \tag{B2}$$

### 2. Neutralino-pairs production

$$\frac{d\hat{\sigma}_{LO}}{d\hat{t}}(b\bar{b}\to\tilde{\chi}_n^0\tilde{\chi}_l^0)$$
$$=\Big(\frac{1}{1+\delta_{nl}}\Big)\frac{4\pi^2\alpha^2}{3s_W^4}\Big[\frac{(g^2_{LZ}+g^2_{RZ})}{c_W^2}(N^R_{nl})^2D_Z^2(2m^2_{\tilde{\chi}_n^0}m^2_{\tilde{\chi}_l^0}+\hat{s}^2+2\hat{s}\,\hat{t}+2\hat{t}^2-(m^2_{\tilde{\chi}_n^0}+m^2_{\tilde{\chi}_l^0})(\hat{s}+2\hat{t})-2m_{\tilde{\chi}_n^0}m_{\tilde{\chi}_l^0}\hat{s})$$
$$+g^2_{bbh}D^2_hS^2_{nlh}(\hat{s}^2-2m_{\tilde{\chi}_n^0}m_{\tilde{\chi}_l^0}\hat{s}-(m^2_{\tilde{\chi}_n^0}+m^2_{\tilde{\chi}_l^0})\hat{s}+g^2_{bbA}D^2_AS^2_{nlA}(\hat{s}^2+2m_{\tilde{\chi}_n^0}m_{\tilde{\chi}_l^0}\hat{s}-(m^2_{\tilde{\chi}_n^0}+m^2_{\tilde{\chi}_l^0})\hat{s})$$
$$+((G^{dL}_{sl})^2+(G^{dR}_{sl})^2)((G^{dL}_{sn})^2+(G^{dR}_{sn})^2)(m^2_{\tilde{\chi}_n^0}-\hat{t})(m^2_{\tilde{\chi}_l^0}-\hat{t})T^2_{\tilde{b}_s}+((G^{dL}_{sl})^2+(G^{dR}_{sl})^2)((G^{dL}_{sn})^2+(G^{dR}_{sn})^2)(m^2_{\tilde{\chi}_n^0}-\hat{u})$$
$$\times(m^2_{\tilde{\chi}_l^0}-\hat{u})U^2_{\tilde{b}_s}+\frac{2N^R_{nl}}{c_W}(G^{dL}_{sl}G^{dR}_{sn}g_{RZ}-G^{dL}_{sn}G^{dR}_{sl}g_{LZ})D_ZT_{\tilde{b}_s}((m^2_{\tilde{\chi}_n^0}-\hat{t})\hat{t}+m^2_{\tilde{\chi}_l^0}(\hat{t}-m^2_{\tilde{\chi}_n^0})+m_{\tilde{\chi}_n^0}m_{\tilde{\chi}_l^0}\hat{s})$$
$$+\frac{2N^R_{nl}}{c_W}(G^{dL}_{sl}G^{dR}_{sn}g_{RZ}-G^{dL}_{sn}G^{dR}_{sl}g_{LZ})\times D_ZU_{\tilde{b}_s}((m^2_{\tilde{\chi}_l^0}-\hat{u})(m^2_{\tilde{\chi}_n^0}-\hat{u})-m_{\tilde{\chi}_n^0}m_{\tilde{\chi}_l^0}\hat{s})-\frac{m_b(m_{\tilde{\chi}_n^0}+m_{\tilde{\chi}_l^0})}{M_W^2}$$
$$\times D_ZD_Ag_{bbA}S_{nlA}N^R_{nl}((m_{\tilde{\chi}_l^0}-m_{\tilde{\chi}_n^0})^2-\hat{s})(2(g_{LZ}-g_{RZ})M_WM_Z-\hat{s})-2g_{bbh}g_{bbH}D_hD_H(\hat{s}^2-(m^2_{\tilde{\chi}_n^0}-m^2_{\tilde{\chi}_l^0})\hat{s}$$
$$-2m_{\tilde{\chi}_n^0}m_{\tilde{\chi}_l^0}\hat{s})+g_{bbh}D_hS_{nlh}\hat{s}\times(G^{dR}_{sl}G^{dR}_{sl}+G^{dL}_{sn}G^{dL}_{sn})((\hat{t}+m_{\tilde{\chi}_n^0}m_{\tilde{\chi}_l^0})T_{\tilde{b}_s}+(\hat{u}+m_{\tilde{\chi}_n^0}m_{\tilde{\chi}_l^0})U_{\tilde{b}_s})$$
$$-g_{bbA}S_{nlA}D_A\hat{s}(G^{dR}_{sl}G^{dR}_{sl}+G^{dL}_{sn}G^{dL}_{sn})((\hat{t}-m_{\tilde{\chi}_n^0}m_{\tilde{\chi}_l^0})T_{\tilde{b}_s}+(\hat{u}-m_{\tilde{\chi}_n^0}m_{\tilde{\chi}_l^0})U_{\tilde{b}_s})+2(G^{dL}_{sl}G^{dL}_{s'l}+G^{dR}_{sl}G^{dR}_{s'l})$$
$$\times(G^{dL}_{sn}G^{dL}_{s'n}+G^{dR}_{sn}G^{dR}_{s'n})[(m^2_{\tilde{\chi}_n^0}-\hat{t})(m^2_{\tilde{\chi}_l^0}-\hat{t})T_{\tilde{b}_s}T_{\tilde{b}_{s'}}+(m^2_{\tilde{\chi}_n^0}-\hat{u})(m^2_{\tilde{\chi}_l^0}-\hat{u})U_{\tilde{b}_s}U_{\tilde{b}_{s'}}]$$
$$-2(m^2_{\tilde{\chi}_n^0}m^2_{\tilde{\chi}_l^0}\mathcal{P}_{\mathrm{nlss}'}+\hat{s}m_{\tilde{\chi}_n^0}m_{\tilde{\chi}_l^0}\mathcal{Q}_{\mathrm{nlss}'}-\hat{t}\,\hat{u}\,\mathcal{R}_{\mathrm{nlss}'})T_{\tilde{b}_s}U_{\tilde{b}_{s'}}\Big] \tag{B3}$$

with

$$D_Z = \frac{1}{\hat{s} - m_Z^2 + i m_Z \Gamma_Z}, \quad D_\phi = \frac{1}{\hat{s} - m_\phi^2 + i m_\phi \Gamma_\phi},$$

$$\text{with } \phi = \mathrm{h}^0, \quad \mathrm{H}^0, \quad \mathrm{A}^0 \tag{B4}$$

$$T_{\tilde{b}_s} = \frac{1}{\hat{t} - m_{\tilde{b}_s}^2}, \qquad U_{\tilde{b}_s} = \frac{1}{\hat{u} - m_{\tilde{b}_s}^2}. \tag{B5}$$

$$\mathcal{P}_{\mathrm{nlss}'} = G_{sn}^{dL} G_{sl}^{dL} G_{s'l}^{dR} G_{s'n}^{dR} + G_{s'l}^{dL} G_{s'n}^{dL} G_{sl}^{dR} G_{sn}^{dR}, \tag{B6}$$

$$\mathcal{Q}_{\mathrm{nlss}'} = G_{sn}^{dL} G_{s'l}^{dL} G_{sl}^{dR} G_{s'n}^{dR} + G_{sl}^{dL} G_{s'l}^{dL} G_{sn}^{dR} G_{s'n}^{dR}, \tag{B57}$$

$$\mathcal{R}_{\mathrm{nlss}'} = G_{s'l}^{dL} G_{s'n}^{dL} G_{sl}^{dR} G_{sn}^{dR} + G_{sl}^{dL} G_{sn}^{dL} G_{s'l}^{dR} G_{s'n}^{dR}. \tag{B8}$$

The factor $1/(1 + \delta_{nl})$ is due to the two identical particles in the final states.


[1] S. L. Glashow, Nucl. Phys. **22**, 579 (1961); S. Weinberg, Phys. Rev. Lett. **19**, 1264 (1967); H. D. Politzer, Phys. Rep. **14**, 129 (1974).
[2] P. W. Higgs, Phys. Lett. **12**, 132 (1964).
[3] P. W. Higgs, Phys. Rev. Lett. **13**, 508 (1964).
[4] P. W. Higgs, Phys. Rev. **145**, 1156 (1966).
[5] F. Englert and R. Brout, Phys. Rev. Lett. **13**, 321 (1964); G. S. Guralnik, C. R. Hagen, and T. W. B. Kibble, Phys. Rev. Lett. **13**, 585 (1964); T. W. B. Kibble, Phys. Rev. **155**, 1554 (1967).
[6] V. D. Barger and E. Ma, Phys. Rev. D **51**, 1332 (1995).
[7] J. R. Ellis, *et al.*, Nucl. Phys. **B238**, 453 (1984).
[8] S. P. Martin, Phys. Rev. D **46**, R2769 (1992).
[9] E. Diehl, *et al.*, Phys. Rev. D **52**, 4223 (1995).
[10] R. Kuchimanchi and R. N. Mohapatra, Phys. Rev. D **48**, 4352 (1993).
[11] R. J. Davis, D. S. Harmer, and K. C. Hoffman, Phys. Rev. Lett. **20**, 1205 (1968); K. S. Hirata *et al.* (KAMIOKANDE-II Collaboration), Phys. Rev. Lett. **65**, 1297 (1990); P. Anselmann *et al.* (GALLEX Collaboration), Phys. Lett. B **327**, 377 (1994).
[12] H. E. Haber and G. L. Kane, Phys. Rep. **117**, 75 (1985).
[13] W. Beenakker, *et al.*, Phys. Rev. Lett. **83**, 3780 (1999); **100**, 029901(E) (2008).
[14] W. G. Ma, *et al.*, Phys. Rev. D **60**, 115009 (1999).
[15] J. Yi, *et al.*, Phys. Rev. D **62**, 035006 (2000).
[16] L. Han, *et al.*, Commun. Theor. Phys. **34**, 115 (2000); A. I. Ahmadov, I. Boztosun, R. K. Muradov, A. Soylu, and E. A. Dadashov, Int. J. Mod. Phys. E **15**, 1183 (2006); G. J. Gounaris, *et al.*, Phys. Rev. D **70**, 033011 (2004); S. Dawson, E. Eichten, and C. Quigg, Phys. Rev. D **31**, 1581 (1985).
[17] J. Debove, B. Fuks, and M. Klasen, Phys. Rev. D **78**, 074020 (2008).
[18] M. Bisset, J. Li, N. Kersting, R. Lu, F. Moortgat, and S. Moretti, J. High Energy Phys. 08 (2009) 037.
[19] H. Baer, *et al.*, Phys. Rev. D **47**, 1062 (1993); H. Baer, *et al.*, Phys. Rev. D **50**, 316 (1994);
[20] F. Moortgat, S. Abdullin, and D. Denegri, arXiv:hep-ph/0112046.
[21] A. Arhrib, R. Benbrik, K. Cheung, and T. C. Yuan, J. High Energy Phys. 02 (2010) 048.
[22] J. M. Lindert, F. D. Steffen, and M. K. Trenkel, J. High Energy Phys. 08 (2011) 151.
[23] G. Bertone, D. Hooper, and J. Silk, Phys. Rep. **405**, 279 (2005); G. Jungman, M. Kamionkowski, and K. Griest, Phys. Rep. **267**, 195 (1996).
[24] J. F. Gunion and H. E. Haber, Nucl. Phys. **B272**, 1 (1986); **B402**, 567(E) (1993); J. F. Gunion and H. E. Haber, Nucl. Phys. **B278**, 449 (1986).
[25] M. M. El Kheishen, A. A. Aboshousha and A. A. Shafik, Phys. Rev. D **45**, 4345 (1992).
[26] A. Djouadi, J. Kalinowski, P. Ohmann, and P. M. Zerwas, Z. Phys. C **74**, 93 (1997); see also, P. M. Zerwas *et al.*, *Report of the Higgs Working Group in the ECFA–DESY Workshop* (1996).
[27] L. J. Hall, R. Rattazzi, and U. Sarid, Phys. Rev. D **50**, 7048 (1994).
[28] M. Carena, *et al.*, Nucl. Phys. **B577**, 88 (2000).
[29] M. S. Carena, *et al.*, Nucl. Phys. **B426**, 269 (1994).
[30] D. M. Pierce, *et al.*, Nucl. Phys. **B491**, 3 (1997).
[31] J. Guasch, P. Hafliger, and M. Spira, Phys. Rev. D **68**, 115001 (2003).
[32] M. S. Carena, *et al.*, Phys. Rev. D **74**, 015009 (2006).
[33] A. Djouadi, Phys. Rep. **459**, 1 (2008).
[34] A. Dedes, *et al.*, Nucl. Phys. **B674**, 271 (2003).
[35] A. Djouadi, *et al.*, Phys. Rev. Lett. **78**, 3626 (1997).
[36] M. Drees and K. Hagiwara, Phys. Rev. D **42**, 1709 (1990).
[37] K. Nakamura *et al.* (Particle Data Group), J. Phys. G **37**, 075021 (2010).
[38] J. A. Casas, A. Lleyda, and C. Munoz, Nucl. Phys. **B471**, 3 (1996); J. M. Frere, D. R. T. Jones, and S. Raby, Nucl. Phys. **B222**, 11 (1983).M. Claudson, L. J. Hall, and I. Hinchliffe, Nucl. Phys. **B228**, 501 (1983); C. Kounnas, *et al.*, Nucl. Phys. **B236**, 438 (1984); J. F. Gunion, H. E. Haber, and M. Sher, Nucl. Phys. **B306**, 1 (1988); P. Langacker and N. Polonsky, Phys. Rev. D **50**, 2199 (1994).C. Le Mouel and G. Moultaka, Nucl. Phys. **B518**, 3 (1998).
[39] S. Heinemeyer, W. Hollik, and G. Weiglein, Comput. Phys. Commun. **124**, 76 (2000).
[40] P. M. Nadolsky *et al.*, Phys. Rev. D **78**, 013004 (2008).

[41] R. Brock *et al.* (CTEQ Collaboration), Rev. Mod. Phys. **67**, 157 (1995); P. M. Nadolsky *et al.*, Phys. Rev. D **78**, 013004 (2008); J. Pumplin *et al.*, J. High Energy Phys. 07 (2002) 012.

[42] S. G. Gorishnii, *et al.*, Mod. Phys. Lett. A **5**, 2703 (1990); , Phys. Rev. D **43**, 1633 (1991); A. Djouadi, M. Spira, and P. Zerwas, Z. Phys. C **70**, 427 (1996); M. Spira, Fortschr. Phys. **46**, 203 (1998).

[43] S. Chatrchyan *et al.* (CMS Collaboration), Phys. Rev. Lett. **106**, 231801 (2011).

[44] D. Benjamin *et al.* (Tevatron New Phenomena Higgs Working Group Collaboration), arXiv:1003.3363.